Probabilistic analysis of serviceability of a grandstand under dynamic crowd loading

Jelle Knibbe [1, 2], Rein de Vries [2, 3], Raphael Steenbergen [2, 4]

[1] Delft University of Technology, Faculty of Technology, Policy and Management, Delft, the Netherlands

[2] Netherlands Organisation for Applied Scientific Research (TNO), Reliable Structures, Delft, the Netherlands

[3] Delft University of Technology, Faculty of Civil Engineering and Geosciences, the Netherlands

[4] Ghent University, Faculty of Engineering and Architectures, Ghent, Belgium

In this paper, a novel method is developed for determining the reliability of a complex structure under dynamic crowd loading, combining a Finite Element model of a structure and a frequency-domain load model in a reliability analysis. The method is applied on a representative case of a grandstand under dynamic crowd loading. Excited crowds jumping up and down on a grandstand can cause noticeable vibrations, which negatively affect the serviceability of the structure due to discomfort. The FE model consists of linear beam elements, with a distributed dynamic load along the seating deck, described in the frequency domain. The amplitude spectrum of this load is parameterized using a number of stochastic parameters, of which the distribution is determined by sampling a dataset of experimentally measured crowd loads. With this load model, the amplitude spectrum of the acceleration response of the grandstand is determined, from which a serviceability criterion based on acceleration intensity is evaluated. Through a Monte Carlo analysis, an exceedance probability P_f of 0.3264 is calculated, with a coefficient of variation of 0.025. A more advanced reliability calculation method, DARS, was also applied, resulting in a value of P_f between 0.400 and 0.444.

Keywords: Structural dynamics, crowd loads, finite element model, reliability, serviceability

1 Introduction

Complex structures under dynamic loads represent a challenge from a structural reliability perspective. Assessing structural performance in such cases is generally arduous, as both the load and structure are difficult to describe, and are affected by uncertainties. This paper presents a novel combination of three different approaches: a frequency-domain load model of a specific type of dynamic load, a finite element model of a structure, and a reliability analysis based on the dynamic response of the structure to the loads. As both models contain quantified uncertainties, the response is also uncertain, meaning its value can be used in the limit state function underlying the reliability analysis. This combined approach is demonstrated with a representative case of a large cantilevered grandstand loaded by jumping crowds.

Crowds jumping up and down on grandstands can cause the seating deck to vibrate noticeably, causing discomfort to the spectators: a serviceability problem. Both this dynamic crowd load and the structure itself are subject to many uncertainties that need to be quantified to assess the safety and serviceability of a grandstand. Therefore, this study presents a combination of a grandstand model and a model of dynamic crowd loads, with uncertainty quantified in both.

The response of this modeling 'train' is then also uncertain, and can thus be used to perform a reliability analysis. This forms a new method for determining the serviceability of a cantilever grandstand under dynamic crowd loading, which is demonstrated using a case study based on a fictitious but representative grandstand structure.

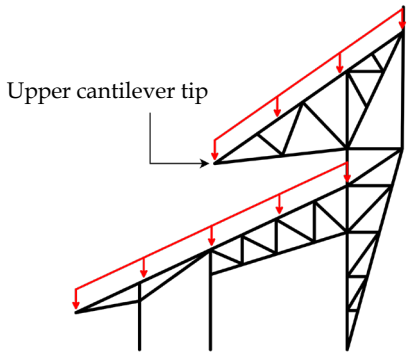

Figure 1. Diagram of a truss in a stadium, with the loaded seating decks and critical location for vibrations indicated

A diagram of this structure is given in Figure 1. Both the loads on the structure and its response to these loads are defined in the frequency domain. For the former, a novel model is used which represents groups of spectators jumping on the two seating decks. Using the mass, stiffness, and damping matrices of a Finite Element model of the structure, the amplitude response spectrum of the accelerations at the tip of the upper cantilever (where the most intense vibrations can be expected) is calculated. This is then used to evaluate a serviceability criterion.

2 Background

*2.1 **Dynamic crowd loads***

Dynamic crowd load is the load generated by crowds jumping, dancing or bobbing (bouncing without leaving the ground) on a grandstand structure, with jumping assumed to be the activity causing the most critical loads. A distinction can be made between rhythmic and non-rhythmic loading, as done by Ellis and Littler (2004), where the former is more synchronized than the latter, and thus more likely to cause resonance. So, this paper concentrates on rhythmic crowd loads.

In the frequency domain, these loads can be characterized as having clear peaks at the jumping frequency and its integer multiples, as if described by a Fourier series. Based on earlier work by (Bachmann et al., 1995), Ellis and Littler proposed the following simple model for Rhythmic Crowd Loading coming from a single person, as a point load (Ellis and Littler, 2004):

$$F(t) = G_s\left(1.0 + \sum_{n=1}^{\infty} r_n \sin(2\pi n\, f_b\, t + \phi_n)\right) \tag{1}$$

where G_s is the weight of the person and f_b is the base jumping frequency of the load, which can vary from 1.0 to 2.8 Hz for jumping according to (Ginty et al., 2001). For a crowd, the weight G_s is replaced by the density of the crowd $G(x,y)$, defining a distributed load. The amplitude r_n and ϕ_n of the n^{th} harmonic could indeed be regarded as forming the Fourier series of the load signal. Usually, the summation of harmonics is truncated to three components. In measured crowd loads (Xiong and Chen, 2021), there is some spread around the peaks in the load spectrum, due to not all spectators jumping at exactly the same frequency, which this model does not take into account.

2.2 *Serviceability of grandstand structures*

Several building codes have been found containing methods to quantify the intensity of the vibrations experienced by a crowd and a grandstand, most notably ISO 2631 on Evaluation of human exposure to whole-body vibration (Canadian Commission on Building and Fire Codes, 2006; International Organization for Standardization, 2007; The Institution of Structural Engineers, 2008). The measure to quantify the 'intensity' of vibrations most often used in these codes is the root-mean-square of the acceleration (RMS), which is based on the perception of vibrations occurring at a specific moment:

$$a_{rms}(t) = \sqrt{\frac{1}{T_s}\int_{t}^{t+T_s} a_w^2(t)dt} \tag{2}$$

where T_s is a sampling period, and $a_w(t)$ is an acceleration record. Before calculating the RMS value, weight factors are applied to the acceleration record based on the frequency of the vibrations (hence the subscript). This weighting, which is similar to a band-pass filter, is applied because humans only perceive vibrations in a certain frequency range (Jones et al., 2011). A table of weighting factors is given in ISO 2631, with different values for the vertical and horizontal directions (See also Figure 10). Another ISO standard, 10137:2007, covering vibrations of buildings and walkways (International Organization for Standardization, 2007), recommends values for the sampling period T_s : 10 seconds for comfort criteria, and 1 second for panic. The shorter this period, the more $a_{rms}(t)$ becomes sensitive to short peaks in the acceleration signal. If T_s is taken as the length of the entire acceleration signal, the RMS is equal to the square root of the power of the signal. The unit of the RMS vibrations is the same as the original acceleration record, often expressed as a percentage or fraction of the gravitational acceleration g. The same holds for the limit values recommended by the norms, (The Institution of Structural Engineers, 2008) for example recommends a maximum of 0.2 g = 1.962 m/s^2 for a design scenario with very active crowds.

2.3 *Reliability Quantification*

In order to quantify the probability-based serviceability of the structure, the probability P_f of not meeting the serviceability criterion needs to be determined. Many criteria, both safety and serviceability, can be formulated in terms of a 'resistance' R and a 'solicitation@ S. A criterion is met when $R > S$. This can be expressed as a limit state function (LSF):

$Z = g(\boldsymbol{X}) = R - S$, where a negative value indicates not meeting the criterion. The input $\boldsymbol{X}$ is formed by the stochastic variables describing the uncertainty in both the resistance and solicitation. The joint distribution function of these variables, $f_{\boldsymbol{X}}(\boldsymbol{x})$ can then be used to calculate the probability of not meeting the criterion P_f as follows (Ditlevsen and Madsen, 2005):

$$P_f = P[g(\boldsymbol{X}) < 0] = \int_{g(\boldsymbol{X})<0} f_{\boldsymbol{X}}(\boldsymbol{x}) d\boldsymbol{x} \tag{3}$$

Evaluating this integral analytically can often become intractable, especially if many stochastic variables are used, if the limit state $g(\boldsymbol{X}) = 0$ has a complicated shape, or if the LSF does not have an explicit formulation (it is a 'black box'). Multiple methods exist to solve this, referred to as reliability methods. Three are highlighted here: crude Monte Carlo (CMC), directional sampling (DS), and directional adaptive response surface sampling (DARS). The latter is an advanced reliability method developed to reduce the number of times the LSF is evaluated. This is advantageous when each evaluation is computationally demanding, for example when it involves running a finite element model (Waarts, 2000).

2.3.1 Crude Monte Carlo

In Crude Monte Carlo (CMC), random sample values for $\boldsymbol{X}$ are drawn according to their joint distribution $f_{\boldsymbol{X}}(\boldsymbol{x})$. The sign of the corresponding output values $g(\boldsymbol{X})$ then determines whether a sample lies in the 'failure' domain of the integral in Equation 3 ($g(\boldsymbol{X}) < 0$). With enough samples, the distribution of the sampled values will resemble $f_{\boldsymbol{X}}(\boldsymbol{x})$, see Figure 2. The resulting P_f is then simply the percentage of simulated values of $g(\boldsymbol{X})$ located in the 'failure' domain. Because CMC considers purely the input $\boldsymbol{X}$ and output $g(\boldsymbol{X})$ of the LSF, and does not require the calculation of derivatives or points lying on the limit state, nor transformation to U-space (see the next paragraph), implementing it is straightforward even for complicated Limit State Functions. The downside is that the method requires a large number of evaluations of the LSF, which may involve running a finite element model or other lengthy calculation, making CMC inapplicable for some reliability problems.

2.3.2 Directional sampling and DARS

Directional sampling (Waarts, 2000) is more complicated than CMC. It involves two transformations of the variables in $\boldsymbol{X}$. First, they are transformed such that their joint distribution is described by several standard normally distributed variables, contained in

the vector $\boldsymbol{U}$. In this U-space, all points located at a certain distance from the origin have the same joint probability $f_{\boldsymbol{U}}(\boldsymbol{u})$. Second, the variables in U-space are transformed to polar coordinates: a direction θ and a distance from the origin λ. Next, directions θ_i are sampled from a uniform distribution. For each of these, the distance λ_i along the direction at which the limit state function is zero in U-space is found (a root). For each root λ_i, a sample probability P_i can be calculated using the CDF of the χ^2_N-distribution, noted as $F_\Lambda(\lambda)$, with the number of degrees of freedom N equal to the number of variables in U-space:

$$P_i = 1 - F_\Lambda(\lambda_i^2) \tag{4}$$

The final probability is then simply the average of P_i over all directions sampled.

A further development of directional sampling is directional adaptive response surface sampling, or DARS. To reduce the number of LSF evaluations needed, a quadratic response surface (RS) is used in directions where λ_i is large, and P_i therefore small, resulting in λ_{RS}.

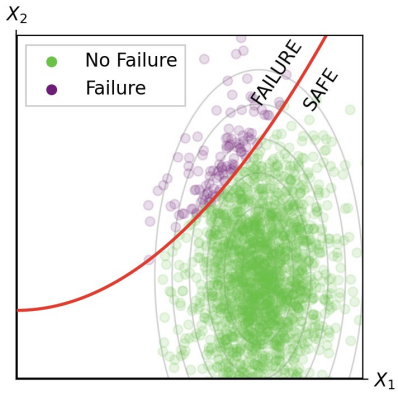

Figure 2. Example of a Crude Monte Carlo analysis

If λ_i is small, which indicates a critical region in U-space, the original LSF is used, and the resulting root point λ_{LSF} is used to update the response surface, improving its accuracy around the critical region (see Figure 3). This way, much less computational effort is needed to find 'far' roots that contribute relatively little to the final result, without sacrificing accuracy for the 'closer' roots in the most critical region in the U-space. The region in which the LSF is used is determined by the smallest root found λ_{min}, and the user-set parameter λ_{add}.

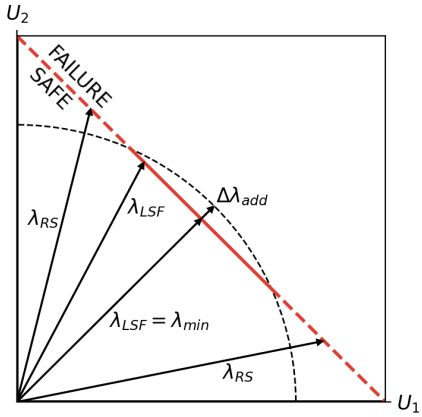

Figure 3. Example of a DARS analysis. λ_{add} is a parameter determining the region in which the LSF (solid line) is used instead of the response surface (dashed line) to find roots.

2.4 ***Synthesis***

Grandstands are complex structures where dynamic properties can play an important role. In order to adequately determine the response to certain loads, finite element models are therefore an attractive approach. However, when the reliability with respect to dynamic loads is considered, the computational costs can become prohibitive. For a load defined in the time domain, the response of the structure for every time step has to be calculated in order, which by itself can be time-consuming. This then has to be repeated many times, depending on the applied reliability method, which makes performing a reliability analysis practically difficult. An advantage of frequency-domain load models is that the response to the load can be calculated for each frequency independently. In a computational setting such as a finite element analysis, this means that the calculations can be parallelized, resulting in a shorter running time (in a reliability calculation, evaluations of the LSF can be parallelized as well. Parallelizing within finite element software may be more convenient to implement, however). As mentioned, the crowd load model of Ellis and Littler describes a Fourier series, meaning it can already be interpreted as a frequency-domain model. Furthermore, the RMS acceleration can also be calculated in the frequency domain using Parseval's theorem, when T_s is equal to the length of the considered signal. This means that the intensity of the accelerations of the structure in response to dynamic crowd loads can, in principle, be determined purely in the frequency domain.

Stochastic models for several types of dynamic loads have been developed in the past, for example for wind and wave loads by Ditlevsen (2002). For the assessment of certain

damages, notably fatigue, frequency-domain models have also been used previously (Muñiz-Calvente et al., 2022), including uncertainty as well (Böhm and Benasciutti, 2021). However, a frequency domain load model of dynamic crowd loads which also takes uncertainties into account does not yet exist. This is needed to perform a reliability analysis, so a novel load model defining the amplitude spectra of a dynamic crowd load is presented in this study.

3 Finite element model

Before the new load model is explained, first the finite element model within which it will be applied is presented. This model represents the truss shown in Figure 1. It forms part of the case study demonstrating the new method, together with the new load model and serviceability criterion, presented in the following two sections.

The model uses quadratic (three-node) Timoshenko beam elements for all members, including the seating deck, with linear elastic material models. The choice for Timoshenko elements was made mostly out of convenience, as these elements were easier to implement in the finite element software used compared to Euler-Bernoulli elements. Most members are modeled by one such element, except some long members in the back of the spine, and the seating deck and the member below it. For the spine, this has been done to make the spacing between nodes somewhat more consistent in the upper part of the truss. For the decks, this is done to split them in a number 'load blocks' of approximately equal length, which are used to apply the dynamic crowd load. Figure 4 shows the mesh of the finite element model.

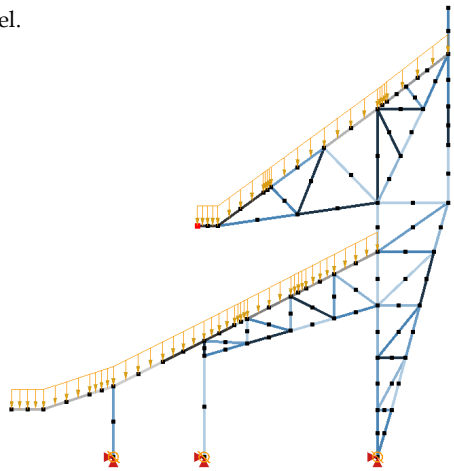

Figure 4. Mesh of the FE model, showing the elements and nodes

Two loads are applied on the modeled truss. These are the static self-weight $\boldsymbol{f}_{\mathrm{st}}$ and dynamic crowd load $\tilde{\boldsymbol{f}}_{\mathrm{crowd}}(f)$. The latter is applied as a distributed load on the seating deck of the trusses, where each load block can have a different value. How these values differ is explained in a following section, covering the crowd load model. To obtain the response to the dynamic load, the static load is used to determine the tangent stiffness matrix $\boldsymbol{K}_t$, similarly to (Magalhães et al., 2008), which is then used in calculating the response to the dynamic load instead of the initial stiffness matrix. The acceleration response $\boldsymbol{a}(f)$ in frequency domain is then calculated as:

$$\tilde{\boldsymbol{a}}(f) = -(2\pi f)^2 [-4\pi^2 f^2 \boldsymbol{M} + 2\pi f i \boldsymbol{C} + \boldsymbol{K}_t]^{-1} \tilde{\boldsymbol{f}}_{\mathrm{crowd}}(f) \tag{5}$$

which also uses the mass matrix $\boldsymbol{M}$ and damping matrix $\boldsymbol{C}$, both calculated using the FE model.

3.1 Modal properties of the structure

The first two mode shapes calculated using the tangent stiffness matrix are given along with the corresponding natural frequencies in Figure 5. The first natural frequency is nearly 2.0 Hz, which is chosen as the target jumping frequency f_{target} for the crowd loads. This means the considered load case will cause resonance, and a significant response can be expected. The corresponding mode sees the truss move mainly in the horizontal direction. The second mode is located at 4.6 Hz and shows more vertical displacement, especially in the upper tier. The mode shapes also indicate that the tip of the upper cantilever can indeed be expected to vibrate significantly, in both vertical and horizontal direction.

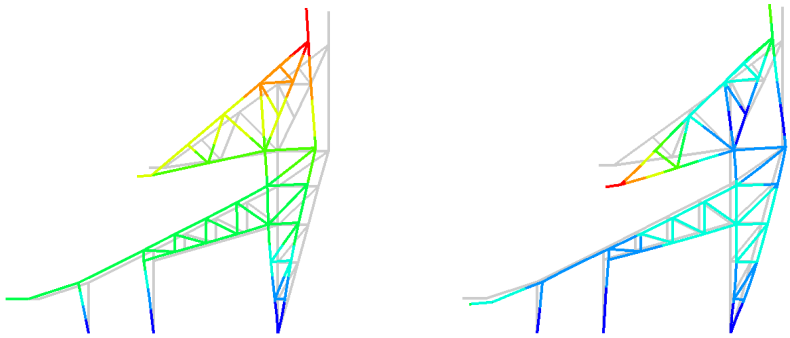

(a) Mode 1: 1.98 Hz *(b) Mode 2: 4.63 Hz*

Figure 5. First two modes of the modelled truss. The colors indicate (relative) total displacements

3.1.1 *Stochastic Variables of the FE Model*

Two distributions have been found for the Young's Moduli of concrete and steel, which influence the stiffness matrix $\boldsymbol{K}$. Gamma-distributions are used, from (Blondeel et al., 2018), who defined these with a shape parameter α and a *scale* parameter β (note that other definitions use a *rate* parameter $1/\beta$): Table 1 shows the values of these parameters as applied in this work, corrected for the units used in DIANA. For the modal properties in the previous section, the mean values of these distributions have been used. Model uncertainty is neglected.

Table 1. Gamma-distributed structure parameters

parameter	unit	α	$1/\beta$
E_s	N/mm²	934.2	4.673×10^{-3}
E_c	N/mm²	7.1633	2.388×10^{-4}

3.2 ***Damping***

The damping matrix $\boldsymbol{C}$ defined using the Rayleigh method:

$$\boldsymbol{C} = a_0\boldsymbol{M} + a_1\boldsymbol{K} \tag{6}$$

where the damping constants α_0 and α_1 are calculated based on the first two natural frequencies and damping ratios, which are estimated as 0.05 for both modes. Uncertainty is not considered for the damping matrix. Human-structure interaction, which could add extra damping to the system, is also ignored (Ellis and Ji, 1997; Weijs, 2023).

4 Crowd load model

This section describes the new frequency-domain load model used to perform the reliability analysis. First, a dataset that is used for fitting the model is presented, followed by a description of the parameterized amplitude spectrum of the rhythmic crowd loads that forms the core of the load model. After that, the quantification of the uncertainty in the parameters is explained. Finally, the application of the load model on the finite element model, as part of the 'modeling train', is described.

4.1 *Crowd load dataset*

A frequency-domain model for dynamic crowd loads has been developed, using a dataset of experimentally measured crowd loads from Xiong and Chen, 2021. This thesis uses the data of 'Experiment IV', where groups of 48 Chinese students were instructed to jump up and down, and the loads of every individual were measured. During these measurement sessions, one of several types of stimuli was used to instruct the students, including popular songs and metronomes set at different frequencies. The dataset contains 204 usable records of students jumping at a metronome frequency of 2 Hz. As mentioned, this is near the first natural frequency of the modeled truss, and thus set as the target jumping frequency, f_{target}. In other words, a scenario is modeled where all spectators on the grandstand section supported by the truss are attempting to jump at 2 Hz, like the students in these records. As such, these 206 records will be used to fit the model and quantify its uncertainties. Herein lies the (conservative) assumption that every spectator is jumping as if they were guided by a metronome, which could be easier to follow than, for example, a song with a similar BPM.

4.2 *Parameterized amplitude spectrum*

The model describes the dynamic crowd load in the frequency domain, through the amplitude spectrum $\left|\tilde{\mathbf{f}}_{\text{crowd}}(f)\right|$, with f as the frequency in Hz. This spectrum consists of a series of 3 peaks $\boldsymbol{P}_k(f)$ (with k = 1, 2, 3) located at integer multiples of f_{target}. Each peak is described by three parameters: $\boldsymbol{H}_k$, $w_{\text{left},k}$ and $w_{\text{right},k}$. The peak height $\boldsymbol{H}_k$ is the value of the spectrum at $f = k\,f_{\text{target}}$. The peaks have tails with a quadratic shape, with the value of $\left|\tilde{\mathbf{f}}_{\text{crowd}}(f)\right|$ reducing from $\boldsymbol{H}_k$ to 0 over their widths $w_{\text{left},k}$ and $w_{\text{right},k}$. Figure 6 shows an example of such a peak, and an example of a complete amplitude spectrum is given in Figure 7.

The model amplitude spectrum of the load can be expressed analytically as follows:

$$\left|\tilde{\mathbf{f}}_{\text{crowd}}(f)\right| = \sum_{k=1}^{3} \boldsymbol{P}_k(f) \;\forall\, f > 0 \tag{7}$$

$$\boldsymbol{P}_k(f) = \begin{cases} \boldsymbol{H}_k \left(\dfrac{f - k\,f_{\text{target}} + w_{\text{left},k}}{w_{\text{left},k}} \right)^2 & \forall f \in [k\,f_{\text{target}} - w_{\text{left},k},\, k\,f_{\text{target}}] \\ \boldsymbol{H}_k \left(\dfrac{f - k\,f_{\text{target}} + w_{\text{right},k}}{w_{\text{right},k}} \right)^2 & \forall f \in [k\,f_{\text{target}},\, k\,f_{\text{target}} + w_{\text{right},k}] \end{cases} \tag{8}$$

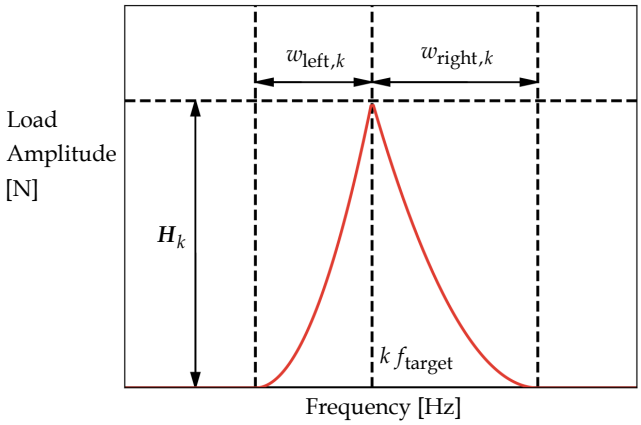

Figure 6. Explanation of the shape of the peaks in the model load spectrum

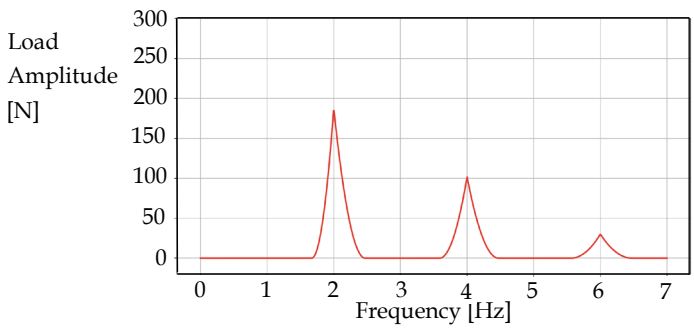

Figure 7. Example of a parameterised load spectrum with 3 peaks

*4.3 **Uncertainty in the load model parameters***

The peak heights and widths are stochastic variables, with lognormal distributions based on the aforementioned dataset of crowd loads (Xiong and Chen, 2021). This sampling was performed as follows: It is assumed that each load block on the upper tier of the grandstand contains 48 jumping spectators. So, 48 of the 204 load records are drawn randomly from the dataset (similar to bootstrapping), then summed, and converted to frequency domain using the fast Fourier transform (FFT) to construct a single 'sample spectrum.' A model amplitude spectrum is then fitted on this sample spectrum, resulting in one value for each of the parameters. This process is repeated 10,000 times, sampling different records from the dataset each time, resulting in 10,000 values for each of the parameters in the load model. A similar process was followed for the lower tier, where 60 spectators are assumed per load block, so 60 samples were taken from the dataset each time. This results in the distributions described by Tables 2 and 3 and Figures 8 and 9. Some slight negative correlations ($\rho \approx -0.3$) between the peak heights and widths could be

observed in the sampled values. This means that tall peaks tended to be thinner, and wide peaks tend to be lower. These correlations are ignored out of convenience, however, meaning that the spectra are slightly overestimated.

Table 2. Lognormally Distributed Load Parameters
for the upper tier with 4 rows (48 spectators) per load block

parameter	unit	μ (m)	σ (s)	ε
$\boldsymbol{H}_{1,48}$	N	188.48	84.95	3.02
$\boldsymbol{H}_{2,48}$	N	102.28	40.42	7.81
$\boldsymbol{H}_{3,48}$	N	30.81	11.23	2.90
$w_{\text{left},1,48}$	Hz	0.3299	0.1862	−0.1644
$w_{\text{left},2,48}$	Hz	0.4075	0.2217	−0.5468
$w_{\text{left},3,48}$	Hz	0.4401	0.2360	−0.9288
$w_{\text{right},1,48}$	Hz	0.4728	0.2309	−2.2520
$w_{\text{right},2,48}$	Hz	0.4872	0.2489	−2.6783
$w_{\text{right},3,48}$	Hz	0.4867	0.2621	−1.3674

Table 3. Lognormally Distributed Load Parameters
for the lower tier with 5 rows (60 spectators) per load block

parameter	unit	μ (m)	σ (s)	ε
$\boldsymbol{H}_{1,60}$	N	220.56	97.64	−1.56
$\boldsymbol{H}_{2,60}$	N	119.00	46.43	6.95
$\boldsymbol{H}_{3,60}$	N	36.12	13.02	2.42
$w_{\text{left},1,60}$	Hz	0.3286	0.1884	−0.1429
$w_{\text{left},2,60}$	Hz	0.4049	0.2215	−0.5246
$w_{\text{left},3,60}$	Hz	0.4366	0.2352	−0.8804
$w_{\text{right},1,60}$	Hz	0.4745	0.2314	−2.6973
$w_{\text{right},2,60}$	Hz	0.4858	0.2479	−2.6737
$w_{\text{right},3,60}$	Hz	0.4852	0.2626	−1.2112

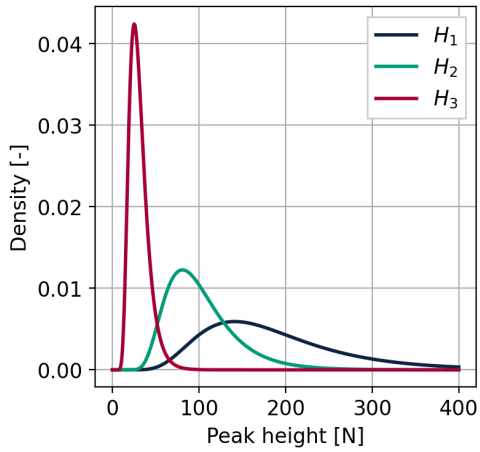

Figure 8. Distribution of the heights of the peaks in the load spectrum model for the upper tier

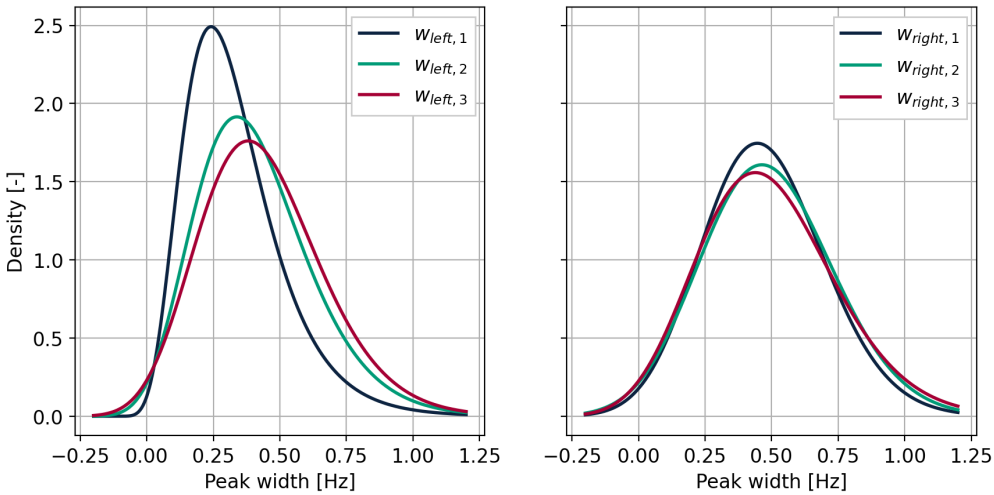

Figure 9. Distribution of the widths of the peaks in the load spectrum model for the upper tier

4.4 *Applying the loads in the FE model*

The load model is applied as follows: For each of the load blocks in the truss, a realization of the parameterized amplitude model is generated, representing the number of spectators in the load block: four (upper tier) or five (lower) rows of twelve spectators. This spectrum is multiplied by a correction factor of 1.3 to account for the weight differences between Dutch men and the Chinese students participating in creating the dataset (WorldData, 2020), and divided by the length of the load block along the seating deck to apply it as a distributed load in the FE model. Finally, a random phase angle is drawn according to a

normal distribution from (Chen et al., 2019), to account for slight phase differences between spectators. While the full phase spectrum is not defined by this load model, this random draw gives a full definition of $\tilde{\mathbf{f}}_{\text{crowd}}(f)$, from which the acceleration response $\tilde{\boldsymbol{a}}(f)$ of the FE model can be obtained.

Not defining the full phase spectrum does have important consequences, however. While the amplitude response spectrum $|\tilde{\boldsymbol{a}}(f)|$ can be calculated accurately, as this depends only on the amplitude spectrum of the load, the same cannot be said for the phase response spectrum. Because of this, transforming the response back to the time domain by combining these two spectra in an inverse Fourier transform does not yield usable results. This means that the current implementation of the model can only be used to assess criteria defined by amplitude response spectra. One such criterion, which will be used to demonstrate the new method and complete the modeling 'train', is covered in the next section. Model uncertainty is neglected.

5 Serviceability Criterion: Exceedance of RMS vibration limit

As mentioned, many criteria can in general be represented by a Limit State Function (LSF) $Z = R - S$: where R is the resistance and S is the solicitation, which is calculated based on the response of the model:

$$S = s(\boldsymbol{X}) + \varepsilon_{\text{phase}} \tag{9}$$

Here $\boldsymbol{X}$ represents the stochastic input parameters of the model, presented in Tables 1, 2 and 3. The function $s(.)$ represents the output, which has random noise $\varepsilon_{\text{phase}}$ added to it due to the phase differences between the load blocks. For this paper, the serviceability criterion concerns the Root-mean-square (RMS) of the acceleration of the tip of the upper cantilever, which may not exceed a deterministic limit defined by a norm. This means S is the RMS of the acceleration, and R is the norm value, and P_f can also be referred to as exceedance probability.

The RMS can be calculated as follows in time domain (Jones et al., 2011):

$$a_{\text{rms}}(t) = \sqrt{\frac{1}{T_s}\int_{t}^{t+T_s} a_w^2(t)dt} \tag{10}$$

where $a_w(t)$ is a frequency-weighted acceleration record and T is a sample time. When T_s is taken as the entire length of the acceleration record, the RMS corresponds to the square root of the power of this signal. Through Parseval's theorem, the power can be calculated in the frequency domain by taking the integral of the square of the amplitude spectrum. Effectively, the acceleration is then assumed to be a periodic function of infinite length ($T_s = \infty$):

$$a_{\mathrm{rms},\infty} = \sqrt{\int_0^\infty \left(W(f)\left|\tilde{A}(f)\right|\right)^2 df} \tag{11}$$

The function $W(f)$ represents the frequency-weighting factors, which are taken from a table in ISO 2631 (International Organization for Standardization, 1997) and linearly interpolated. Figure 10 shows these factors. $\tilde{A}(f)$ is the acceleration response spectrum of the specific location and direction being considered. These are specific components of the acceleration response $\tilde{\boldsymbol{a}}(f)$, namely the horizontal and vertical acceleration at the node in the FE model located at the tip of the upper cantilever. According to ISO 2631, both of these should be considered, and to obtain a single RMS value for serviceability they should be combined as follows:

$$s(\boldsymbol{X}) = a_{\mathrm{rms,total}} = \sqrt{a_{\mathrm{rms,vertical}}^2 + a_{\mathrm{rms,horizontal}}^2} \tag{12}$$

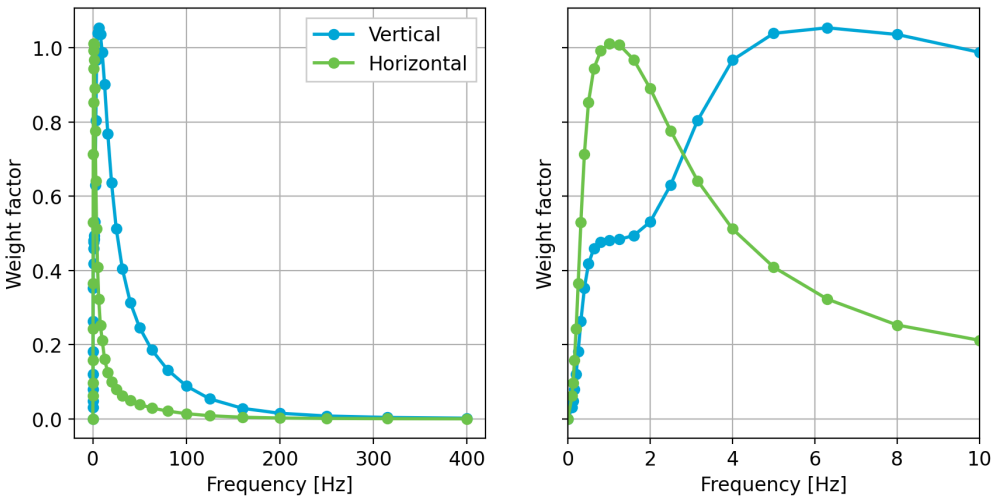

Figure 10. Frequency-weight factors for accelerations
Left: full table from ISO 2631 (International Organization for Standardization, 1997).
Right: zoomed in to the relevant frequency range

5.1 *RMS limit*

Serviceability requirements are generally somewhat subjective. The UK standard mentioned in the Literature Study is focused specifically on grandstands and uses multiple different scenarios with different types of crowds (The Institution of Structural Engineers, 2008). For 'extreme events' with 'vigorous participation' of the spectators, it recommends 20% of the gravitational acceleration g as a limit: 1.962 m/s^2. This deterministic limit is taken as R, though it could in principle be treated as a stochastic variable as well. After all, the tolerance towards vibrations could differ from spectator to spectator. Section 7 briefly discusses how varying vibration tolerances could be treated.

5.2 *Reliability Analysis*

Two Reliability Methods are applied: Crude Monte Carlo and DARS. Multiple DARS analyses are performed with λ_{add} varying. The coefficient of variation $V(P_f)$ to be reached before stopping the analysis is set at 0.05, similar to Waarts, 2000.

Both CMC and DARS obtain an exceedance probability of the RMS limit, P_f , as their main output. Such a probability should generally be interpreted with respect to a reference period (e.g. one year, 50 years, or the expected lifetime of a structure). In this case, it could be described as 'during one instance of *all* spectators jumping and attempting to follow a frequency near the first natural frequency of the structure', which is clearly not as straightforward as a set number of years. A conversion could be made by estimating how often this scenario occurs in, for example, one year. This depends on the type of events being hosted at the stadium, which is not specified in this case study. As such, interpreting the failure probability with respect to time is not further discussed in this paper.

6 Results

6.1 *Crude Monte Carlo*

Figure 11 shows the results of the Crude Monte Carlo analysis in a histogram. The horizontal axis represents the RMS (S) values resulting from the simulations with random draws of $\boldsymbol{X}$, and the vertical axis represents the number of times values within a range occurred. The histogram is cut in two sides by the deterministic limit value 0.2g (R). Of the 5000 simulations performed, 1632 resulted in an RMS value larger than the limit, which

means the limit exceedance probability P_f is found to be 0.3264, with a coefficient of variation of 0.025. Running these simulations took approximately 20 hours on an office laptop. Some time could have been saved if a larger coefficient of variation of the failure probability had been accepted.

6.2 *DARS*

Table 4 below shows the results of the DARS reliability analyses. Here, $V(P_f)$ forms a stopping criterion, and the value to be reached before stopping the analysis was set to 0.05. The value of λ_{add} was varied, and the resulting limit exceedance probability P_f and reliability index β are given for every analysis. Furthermore, the number of evaluations of the LSF and Response Surface is given. The limit exceedance probabilities found by DARS are larger than the value found by Crude Monte Carlo, though within the same order of magnitude. The number of LSF evaluations needed increases with λ_{add} and was generally much less than the 5000 used for the Monte Carlo analysis.

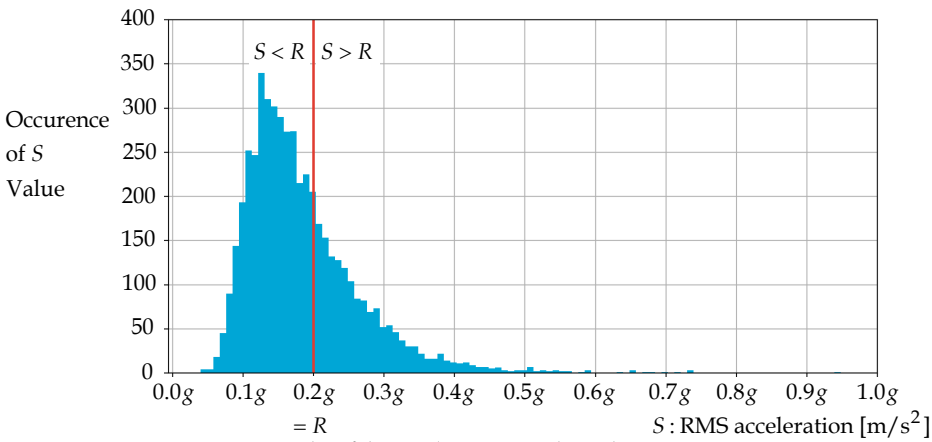

Figure 11. Results of the Crude Monte Carlo analysis

Table 4. Results of the DARS Reliability Analysis

λ_{add}	P_f	β	LSF evaluations	RS evaluations
0.0	0.428	0.182	123	2377
0.1	0.444	0.140	161	2921
0.2	0.400	0.252	186	2503
0.3	0.408	0.233	316	9724
0.4	0.420	0.202	425	13460
0.5	0.417	0.209	519	17083

7 Discussion

Instead of considering a single value for the exceedance probability, based on a single limit, it can be considered as a function of the limit: $P_f(R)$. This is relevant as tolerance towards vibrations is inherently subjective, so one spectator in the stadium may experience discomfort only at larger RMS accelerations than another. It is therefore useful to know how often different values of RMS accelerations can be exceeded.

Figure 12 shows this exceedance probability: for every RMS value simulated through CMC, the percentage of simulations exceeding that value is plotted. This is equivalent to the resulting P_f of a CMC analysis that would have used that RMS value as R. If, hypothetically, a distribution function of vibration tolerances of spectators was known, the exceedance probability for an individual spectator could be calculated. This is somewhat similar to the use of a fragility function, used to assess the response of a structure to dynamic loads such as earthquakes (Baker, 2015), where the probability of collapse is described by a function of the earthquake intensity. Such a vibration tolerance distribution is difficult to construct, however, as this tolerance will depend on many different factors. While the resistance in many limit state functions represents a mechanical or physical aspect (e.g. the yield strength of steel), an individual's tolerance towards vibrations is mostly a psychological aspect.

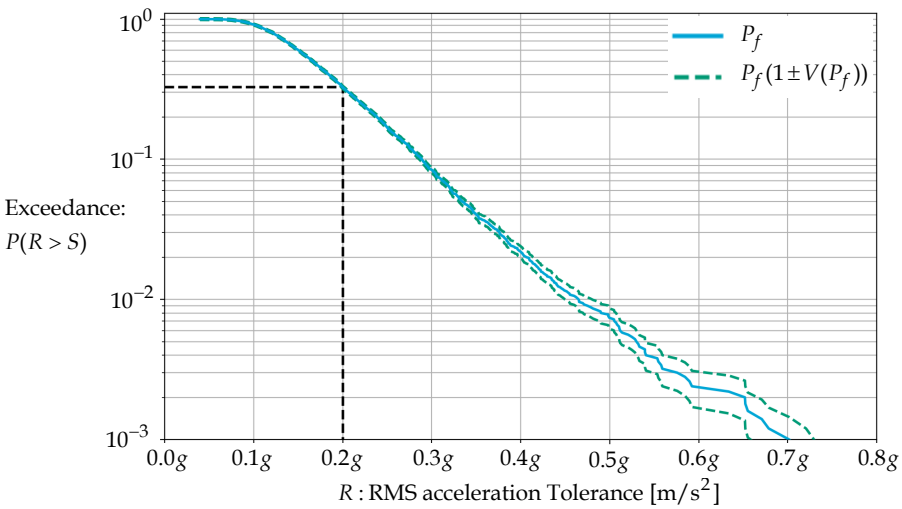

Figure 12. Exceedance probability of RMS values calculated from the CMC results, in semilog scale and with coefficient of variation indicated

It should also be noted that only one location in the truss is being considered, one where the most extreme vibrations could be expected. This means that the majority of spectators will experience less intense vibrations than those calculated by the models, and that their 'individual' exceedance probability will be much smaller.

Additionally, in Figure 12, the coefficient of variation of the failure probability is calculated for every value of R, and used to indicate the accuracy of the estimated exceedance probability. For $R > 0.4g$, $V(P_f)$ becomes larger than 0.1. This shows that the method presented in this paper is able to calculate smaller probabilities with CMC, even values in the order of 10^{-2}, with reasonable accuracy. Smaller values could be reached, but this also requires more LSF evaluations and thus more costly evaluations of the FE model. For much smaller values of P_f, which are expected for safety criteria, a different reliability calculation method requiring fewer LSF evaluations is needed.

DARS could play this role, however, it is likely affected more by the noise $\varepsilon_{\text{phase}}$ in the limit state function than CMC. DARS uses specific, calculated values of $\boldsymbol{x}$ in its root-finding algorithm, while CMC uses randomly generated numbers. As the phase angles are randomly generated in both, they are expected to have a more pronounced effect on DARS than on CMC.

The variation in P_f between the different DARS analyses with different values of λ_{add} is relatively small. Using the average of the six runs $\hat{\mu}_{P_f,DARS}$, which is 0.420, and the $V(P_f)$ to be reached by DARS (set to 0.05), an interval $\hat{\mu}_{P_f,DARS}\ (1 \pm V(P_f))$ similar to those shown in Figure 12 can be established. The lower and upper bounds of this interval are 0.399 and 0.444, respectively. All six individual results fall within this interval (though those with λ_{add} set to 0.1 and 0.2 are close to the bounds), so DARS appears to be able to find a reasonably consistent result for P_f.

This does not explain the difference with the CMC result, which lies far outside this interval. However, it does suggest that $\varepsilon_{\text{phase}}$ introduces a certain degree of bias between the two methods, rather than causing DARS to yield erratic (and unusable) results. Specifically, it appears to cause roots to be found closer to the origin in U-space than they truly are, at least in this case. Further investigation of this hypothesised bias is out of the scope of this paper. Furthermore, rather than quantifying the presumed effects of the noise

caused by the phase angles, it is perhaps more worthwhile to investigate how this noise can be removed altogether.

8 Conclusions and recommendations

This paper presented a novel method of assessing the reliability of a grandstand under dynamic crowd loading. A new frequency domain load model with uncertainties was applied in a Finite Element model of a representative grandstand structure. A serviceability criterion based he vibration response of the grandstand to this load was used to perform a reliability analysis. This final section provides conclusions and recommendations based on this research.

*8.1 **Conclusions***

• The novel frequency domain load model presented in this paper is able to probabilistically represent the amplitude spectrum of the load generated by a jumping crowd.

• By applying this load model on a finite model of a grandstand, the methodology presented in this paper is able to determine failure (or limit exceedance) probability for a serviceability criterion based on the response of a cantilever grandstand loaded by a jumping crowd, provided that the criterion can be evaluated in the frequency domain with the amplitude response spectrum only.

• With a Crude Monte Carlo (CMC) analysis, a failure (or limit exceedance) probability of the order of magnitude 10^{-2} and larger can be found with a number of LSF evaluations requiring 2 to 3 working days of runtime, if one LSF evaluation takes 10 to 16 seconds.

• With a DARS analysis, a failure (or limit exceedance) probability of the same order of magnitude can also be found, though the resulting value is somewhat larger than the Crude Monte Carlo result.

• A DARS analysis requires a much shorter runtime, ranging from 0.5 to 2 hours depending on the chosen λ_{add} . This means DARS is also able to find smaller failure probabilities, for different criteria, in a reasonable amount of time.

• Different criteria, specifically those defined in the time domain, can currently not be applied due to the lack of a model of the phase spectrum.

8.2 Recommendations for further research

Aside from a few conservative assumptions, the main area of improvement for the method presented in this paper lies in the definition of the phase angles in the load model. They should not introduce noise in the limit state function, so for a certain realization $\boldsymbol{x}$ of the stochastic variables in $\boldsymbol{X}$, the value of the LSF $g(\boldsymbol{X} = \boldsymbol{x})$ should always be the same. Furthermore, and likely more challenging, is that the phase angle spectrum in the load model should be representative of that of the measured loads used to construct it.

Alternatively, instead of a load and amplitude spectrum, the load could also be represented by the spectra of its real and imaginary components. Parameterising these may be more difficult than is currently done for the amplitude spectrum, but easier than for the phase spectrum, while still obtaining a full frequency-domain description of the load. In either case, a better load model would allow for more criteria to be considered as part of the reliability analysis, including ones pertaining to safety instead of serviceability.

Acknowledgements

This paper is based on the Master thesis of the author (Knibbe, 2023). More details on the novel reliability methods, especially concerning the load model, can be found there.
The author would like to thank his graduation committee once again, consisting of Eliz-Mari Lourens, Raphaël Steenbergen, Frans van der Meer and Rein de Vries.

References

Bachmann, H., Ammann, W. J., Deischl, F., Eisenmann, J., Floegl, I., Hirsch, G. H., Klein, G. K., Lande, G. J., Mahrenholtz, O., Natke, H. G., Nussbaumer, H., Pretlove, A. J., Rainer, J. H., Saemann, E.-U. & Steinbeisse, L. (1995). *Vibration problems in structures*. Birkhäuser Basel. https://doi.org/10.1007/978-3-0348-9231-5

Baker, J. W. (2015). Efficient analytical fragility function fitting using dynamic structural analysis. *Earthquake Spectra*, 31(1), 579–599. https://doi.org/10.1193/021113EQS025M

Blondeel, P., Robbe, P., Van Hoorickx, C., Lombaert, G. & Vandewalle, S. (2018). Multilevel monte carlo for uncertainty quantification in structural engineering. *CoRR*, abs/1808.10680. https://doi.org/10.48550/arXiv.1808.10680

Böhm, M. & Benasciutti, D. (2021). A frequency-domain model assessing random loading damage by the strain energy density parameter. *International Journal of Fatigue*, 146, 106152. https://doi.org/10.1016/J.IJFATIGUE.2021.106152

Canadian Commission on Building and Fire Codes. (2006). User's guide: Nbc 2005: Structural commentaries (part 4 of division b). (NRCC 48192). https://doi.org/10.4224/40002075

Chen, J., Tan, H., Van Nimmen, K. & Van den Broeck, P. (2019). Data-driven synchronization analysis of a bouncing crowd. *Shock and Vibration*, 2019. https://doi.org/10.1155/2019/8528763

Ditlevsen, O. & Madsen, H. O. (2005, July). *Structural Reliability Methods*. http://www.mek.dtu.dk

Ditlevsen, O. (2002). Stochastic model for joint wave and wind loads on offshore structures. *Structural Safety*, 24(2-4), 139–163. https://doi.org/10.1016/S0167-4730(02)00022-X

Ellis, B. R. & Ji, T. (1997). Human-structure interaction in vertical vibrations. *Proceedings of the Institution of Civil Engineers - Structures and Buildings*, 122(1), 1–9. https://doi.org/10.1680/istbu.1997.29162

Ellis, B. R. & Littler, J. D. (2004). Response of cantilever grandstands to crowd loads. Part 2: Load estimation. *Proceedings of the Institution of Civil Engineers-Structures and Buildings*, 157(5), 297–307. https://doi.org/10.1680/stbu.2004.157.5.297

Ginty, D., Derwent, J. & Ji, T. (2001). The frequency ranges of dance-type loads. *Structural Engineer*, 79(6), 27–31. https : / / research . manchester. ac . uk / en / publications / the - frequency-ranges-of-dance-type-loads

International Organization for Standardization. (1997). Mechanical vibration and shock - evaluation of human exposure to whole-body vibration. (ISO 2631-1:1997).

International Organization for Standardization. (2007). Bases for design of structures — serviceability of buildings and walkways against vibrations. (ISO 10137:2007). https://connect.nen.nl/Family/Detail/28205?compId=10037&collectionId=0

Jones, C., Reynolds, P. & Pavic, A. (2011). Vibration serviceability of stadia structures subjected to dynamic crowd loads: A literature review. *Journal of Sound and Vibration*, 330(8), 1531–1566. https://doi.org/10.1016/j.jsv.2010.10.032

Knibbe, J. (2023). Serviceability of a cantilever grandstand under dynamic crowd loading [Master's thesis, Delft University of Technology]. http:// resolver.tudelft.nl/ uuid: 8379608c-e790-45cb-918c-c93cead6fb3a

Magalhães, F., Caetano, E. & Cunha, Á. (2008). Operational modal analysis and finite element model correlation of the braga stadium suspended roof. *Engineering Structures*, 30(6), 1688–1698. https://doi.org/https://doi.org/10.1016/j.engstruct.2007.11.010

Muñiz-Calvente, M., Álvarez-Vázquez, A., Pelayo, F., Aenlle, M., García-Fernández, N. & Lamela-Rey, M. J. (2022). A comparative review of time- and frequency-domain methods for fatigue damage assessment. *International Journal of Fatigue*, 163, 107069. https://doi.org/10.1016/J.IJFATIGUE.2022.107069

The Institution of Structural Engineers. (2008). Dynamic performance requirements for permanent grandstands subject to crowd action: Recommendations for management, design and assessment. Institution of Structural Engineers. https://www.istructe.org/resources/guidance/dynamic-performance-grandstands-crowd-action/

Waarts, P. H. (2000). *Structural reliability using finite element analysis* [Doctoral dissertation, Delft University of Technology].

Weijs, H. (2023). A reliability assessment of grandstand elements [Master's thesis, Delft University of Technology]. http://resolver.tudelft.nl/uuid:c2dfcb04-9368-412d-9367-bd8337ed0858

WorldData. (2020). Average sizes of men and women. https://www.worlddata.info/averagebodyheight.php

Xiong, J. & Chen, J. (2021). Open access and updated human-induced load data set. *Journal of Structural Engineering*, 147(3), 04720003. https://doi.org/10.1061/(ASCE)ST.1943-541X.0002932